Sub Topic: Laminar Flames

2024 Spring Technical Meeting of the Central States Section of The Combustion Institute
May 12 - 14, 2024
Case Western Reserve University in Cleveland, OH

Flame Speed of Ammonia-Hydrogen Blends at High Gas Temperatures and Pressures

*Julien Douvry-Rabjeau[1], Tushar Goyal[1], Jacob Klein[1], Philip Zoldak[2], Omid Samimi-Abianeh[1] **

[1]Department of Mechanical Engineering, Wayne State University, 5050 Anthony Wayne Dr, Detroit, Michigan, 48202, USA
**Corresponding Author Email: o.samimi@wayne.edu*

1. Introduction

Ammonia (NH_3) has gained attention as a promising carbon-free fuel due to its high energy density [1] and the ability to be stored in liquid form at 1.1 MPa under normal temperature conditions. Despite its relatively low calorific value of 18.8 MJ/kg, NH_3 has found applications as a fuel in various industrial settings such as gas turbines [2]. This makes Ammonia a potential alternative to clean fuels like hydrogen. Researchers have focused their efforts on investigating combustion properties of Ammonia, including its fundamental combustion characteristics, chemical kinetics modeling, and utilization in internal combustion engines and gas turbines, either as a single-component fuel or in multi-component fuel blends [1,3,4]. However, the combustion intensity of Ammonia is notably low, with its laminar flame speed being an order of magnitude lower than that of hydrocarbons at ambient temperature and pressures [2,5]. Improving flame stability is a critical challenge that needs to be addressed for the practical application of ammonia as a fuel.

Several experimental and simulation studies have explored methods to enhance the stability of ammonia flames [2,6–9], with the addition of hydrogen, methane, and carbon monoxide to ammonia-air mixtures proving effective in increasing flame speed and improving flame stability. Pessina et al. [6] developed LFS correlations for NH_3/H_2/Air at elevated pressures (40 – 130 bar), temperatures (720 – 1200 K), and equivalence ratios ranging between 0.4 – 1.5. The results suggested that the increasing mole fraction of hydrogen results in a higher laminar flame speed. Goldmann and Dinkelacker et al. [7] developed an empirical equation capable of predicting LFS under elevated thermodynamic conditions. Li et al. [10] conducted LFS for NH_3/H_2/air mixtures with various volume fractions and equivalence ratios using a Bunsen burner at ambient conditions. Similarly, Han et al. [11] obtained LFS using the heat flux method for NH_3/air mixtures blended with CO, H_2, and CH_4 at 298 K, and 0.1 MPa. Lhuillier et al. [12] experimentally investigated the LFS of NH_3/H_2/air mixtures at different equivalence ratios, hydrogen contents, and temperatures at 0.1 MPa, observing a gradual increase in LFS with increasing H_2 content and initial temperature. Shrestha et al. [13] analyzed the LFS of NH_3/O_2 and NH_3/H_2 mixtures at high temperature and pressure, concluding that elevated initial temperatures could enhance the LFS.

Nonetheless upon reviewing the existing literature, a comprehensive understanding of the combustion characteristics (such as autoignition and laminar flame speed) of NH_3/H_2 blends at engine operating conditions is lacking, hindering its real-world application. Thus, the primary objective of this investigation is to provide high-fidelity LFS measured data for stochiometric NH_3/H_2 at compressed gas pressures of 5 and 10 bar, across broad spectrum temperatures. Furthermore, a comparison between experimental and simulated results using a kinetic mechanism (Chen et al. [14]) was conducted, providing valuable insights for future fuel development and application and improvement in existing kinetic mechanism.

2. Experimental set up

Laminar flame speed (LFS) experiments were carried out at the Combustion Physics Lab of Wayne State University using the Rapid Compression Machine – Flame (RCM-Flame). The RCM-Flame, designed to emulate the compression stroke of an internal combustion engine, compresses gas mixtures through a pneumatically driven piston, which is hydraulically stopped. The combustion was initiated via spark ignition. This device features a combustion chamber with a 10-inch stroke and 2-inch internal diameter. A 0.75-inch thick and 2-inch diameter sapphire optical window was fitted to its front, allowing view into the chamber, and recording of flame propagation. Two opposing horizontally oriented electrodes, separated by 0.8 mm, facilitated spark ignition. Figure 1 graphically depicts the experimental set up for this work.

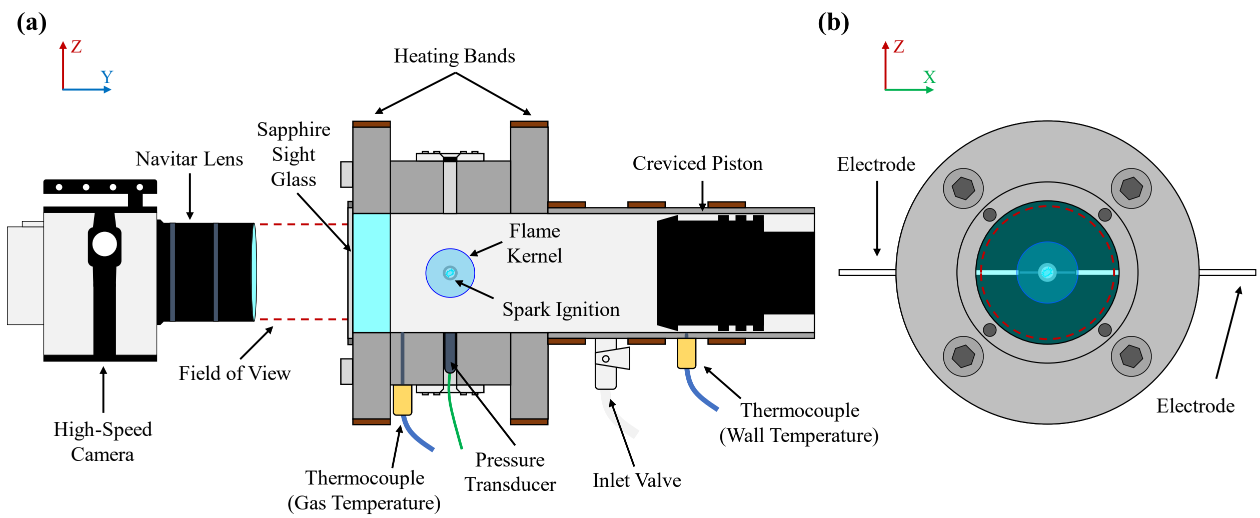

Figure 1. Schematic of the RCM-Flame experimental arrangement

Flame propagation events were captured using a high-speed camera (Vision Research, Phantom VEO-410L) paired with a 50 mm lens (Navitar, DO-5095) was aligned with the sapphire window of the RCM-Flame. Spark ignition was achieved through a 12V DC powered spark energy system, comprising of a variable generator (TekPower, TP3015E), a solid-state relay (VB Controls, PE0630), an ignition coil (MSD Ballast 2), and an ignition capacitor (Duralast, URS1502). The spark was initiated using a laser trigger system (Calpac Lasers, CP-TIM-201-1D-650, 630-680nm and a photodiode, Hamamatsu Silicon Photodiode, S1787-08). The timings for spark ignition and camera recording were governed by a delay generator (Stanford Research Systems, DG646).

The RCM-Flame's gas temperature was monitored using a high-accuracy thermocouple (Omega K-type KMQSS-125G-6, $\pm$ 1.1K). Five K-type thermocouples (Omega, KMQSS-062G-6, associated uncertainty $\pm$ 2.2K) were attached to the RCM-Flame's combustion chamber walls to monitor temperature homogeneity. The gas mixture was prepared with a high-precision static pressure sensor (Omega, PX409-050A10V-EH). The pressure inside the combustion chamber during the compression event was measured using a piezoelectric transducer (Kistler 6045B with

0.56% uncertainty). NI LabVIEW software was used to monitor and record the pressure and temperature data from these sensors.

Gas mixtures were meticulously prepared using NH_3, H_2, O_2, He, Ar, and N_2 (ultra-high purity, 99.9999%) gases sourced from Airgas. Prior to introducing each new gas mixture into the tank or conducting a test in the RCM-Flame, gas residuals were evacuated using a vacuum pump (Agilent, DS202), reaching a pressure of 2 mbar. Once the residual gases were evacuated, the mixture was produced by adding each gas sequentially based on their partial pressure (see, Table 1). To ensure the mixture homogeneity, a minimum of four hours was allotted for mixing, prior to conducting the experiments.

The gas mixtures used in this study are summarized in Table 1. Each experiment was conducted at a fixed equivalence ratio of 1.0. The initial set of mixtures (#1 to #4) consisted of 70%NH_3/30%H_2 blend as fuel, while the mixture #5 consisted of 50%NH_3/50%H_2 and finally mixtures #6 to #8 consisted of pure H_2 as fuel.

Table 1: Mixture composition (partial pressure, bar)

Mixture:	**Composition**					
	H_2	**NH_3**	**O_2**	**N_2**	**He**	**Ar**
1	0.0712	0.1661	0.1602	0	0.6025	0
2	0.0712	0.1661	0.1602	0	0.3013	0.3013
3	0.0712	0.1661	0.1602	0	0.1506	0.4519
4	0.0712	0.1661	0.1602	0	0	0.6025
5	0.1258	0.1258	0.1572	0	0.5913	0
6	0.2958	0	0.1479	0.5563	0	0
7	0.2958	0	0.1479	0.2782	0.2782	0
8	0.2958	0	0.1479	0	0.5563	0

Spherical flame speeds were measured using image analysis of experimental recordings, as detailed in this section. The frame rate and exposure time of the recordings were 20,000 fps and 30µs for NH_3/H_2 flames and 50,000 fps and 10µs for pure H_2 flames. Recordings were segmented into frames and processed in MATLAB [15], employing in-house algorithms to ascertain flame dimensions and positions at each interval, as illustrated in Figure 2. Once the flame radius was determined for each time step, the burning velocity was computed using second order finite difference formulas for numerical differentiation. This methodology has been comprehensively detailed in our previous publications [16].

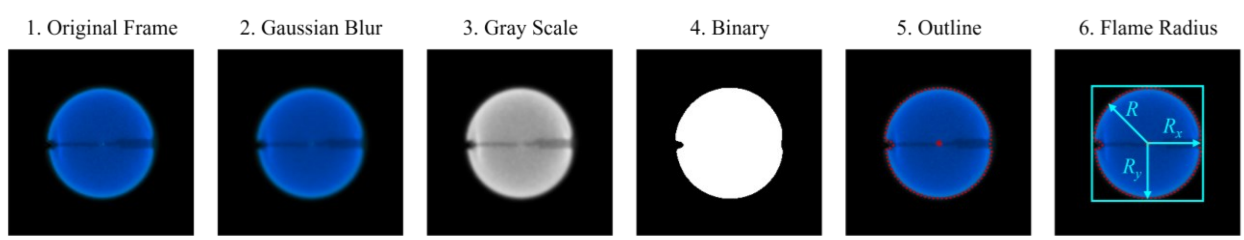

Figure 2. Image processing operations to determine flame location, size, and speed.

To mitigate the effect of spark energy release, confinement effects due to chamber walls, and ensure isobaric conditions, a data processing interval was instituted on the acquired burning velocities (S_b). The flame radius (R) versus stretch rate plot (Figure 3, left) revealed three distinct regions: initial turbulent propagation fueled by spark energy, a quasi-steady state of flame movement, and a deceleration due to the confinement influence [17]. The focus was on the quasi-steady section for determining the unperturbed burning velocity S_b^0. However, to preserve quasi-isobaric conditions, a 7% pressure rise limitation, from the time of spark ignition, was imposed. As an example, the data under quasi-steady segment analyzed for extrapolation is illustrated in the pressure trace of Figure 4.

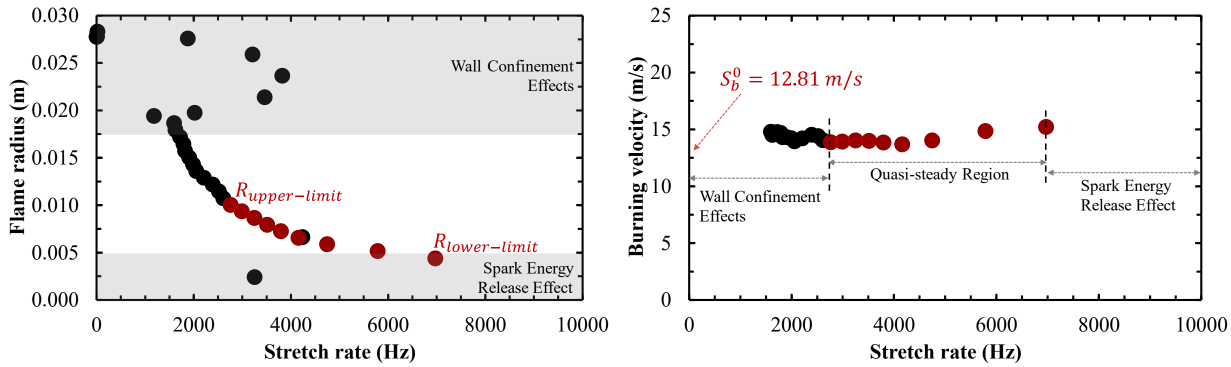

Figure 3. Region of interest for flame speed extrapolation (mixture #5 at 5 bar 666 K)

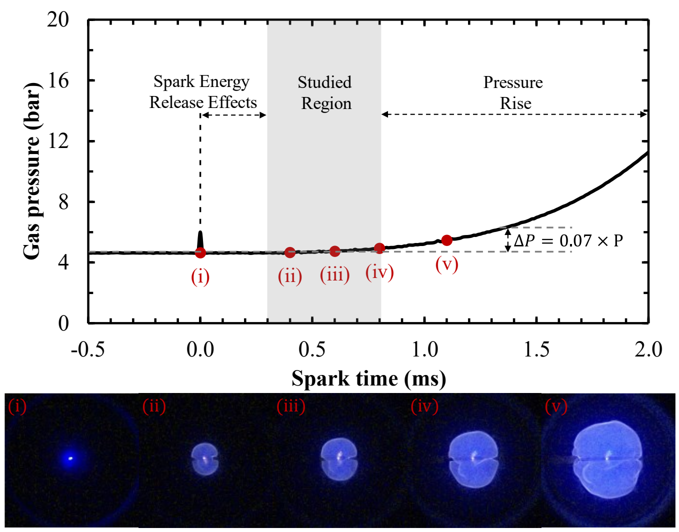

Figure 4. Pressure trace and corresponding flame images (mixture #5 at 5 bar and 666 K)

The data in the propagation region of interest was then fit to the Karlovitz's model:

$$S_b = S_b^0 - L_K K \quad (1)$$

where L_K is a constant to which the stretch response is attributed, and $K=(2/R)/(dR/dt)$ is the stretch rate. Lastly, the laminar flame speed S_u^0 was calculated from S_b^0 using the continuity equation:

$$\rho_u S_u^0 = \rho_b S_b^0 \quad (2)$$

where ρ is the density and the subscripts 'u' and 'b' denote the unburned and burned states, respectively. The densities of the burned and unburned mixture were acquired from simulation as detailed in the next section of this work.

3. Computational Framework

A homogenous charge compression ignition (HCCI) model was utilized to determine gas temperatures during the post-compression and spark initiation, with its accuracy well documented in a previous work [18]. The correlation between initial conditions and properties at the time of spark initiation for the RCM-Flame is presented as:

$$\ln\left(\frac{P_s}{P_i}\right) = \int_{T_i}^{T_s} \frac{\gamma(T)}{\gamma(T)\text{-}1}\frac{dT}{T} \tag{3}$$

where γ is the specific heat ratio of the gas at temperature T and the subscripts $(\cdot)_s$ and $(\cdot)_i$ denote spark time and initial properties, respectively.

In this study, the mechanism proposed by Chen et al. [14] was used to derive simulated flame speeds and intermediate radical concentrations for NH_3/H_2 blends under varying conditions. Flame speeds were predicted using PREMIX module [19] available in Chemkin-Pro. A 150mm-long tube was used to calculate burning velocity. The tube was discretized in 3000 grid point, while 100 points were adaptive points in the mesh along the tube. The maximum gradient allowed between grid points was set to 0.1, while for the maximum curvature allowed was set to 0.5. Finally, the initial grid points were based on temperature profile. This numerical setup allowed a fast calculation of a converged burning velocity.

Following the recommendations of Da et al. [20] and Mathieu and Petersen [21], the evaluation of key intermediate species mole fraction was crucial for accurately determining the density ratio of burned to unburned states. Utilizing the top 10 predicted species, alongside gas pressure and temperature at the time of spark initiation, calculations were made for burned and unburned densities, as well as adiabatic flame temperatures for each experiment. These computations were facilitated by the Equilibrium module in Chemkin-Pro [22]. The obtained density ratio was then applied to the unstretched, burned flame speed, as determined by Eq. (2), to derive the laminar flame speed in the unburned condition. Soret effect was considered for all simulations with mixtures composed of hydrogen.

Uncertainties have been calculated for both measured and simulated data. Those uncertainties include: ±1.1K from thermocouple and ±0.05% from the static pressure sensor for the initial temperature and pressure of the gas mixture before compression. Uncertainty from the piezoelectric transducer has been counted (0.56% uncertainty). The mixture uncertainty has also been considered which changes the equivalence ratio (±0.001). A post compression temperature uncertainty of ±2.5K has been taken into account. An uncertainty of ±3 pixels has been set for the footage recorded with the high-speed camera. The Gaussian blur value has an uncertainty of ±1%. The average uncertainty has been found to be around 5% for the measurements and 2% for the simulations.

4. Results and Discussion

This study aimed to further our knowledge of alternative fuel blends by acquiring experimental NH_3/H_2 flame speed data under elevated thermodynamic conditions. The experiments assessed three stoichiometric NH_3/H_2 blends, conducted at gas pressures of 5 and 10 bar, with gas temperatures ranging from 592 to 706 K.

4.1 Flame speeds of hydrogen-ammonia blends

Figure 5 shows the effect of hydrogen mole fraction in NH_3/H_2 blends on flame speed. An increase in hydrogen concentration (within the total fuel mixture) increases the flame speed. In addition, as the mole fraction of hydrogen in the blend increases (i.e., 30% to 100%), a rise in compressed gas temperature (659 to 685 K at 5bar and 668K to 701K at 10bar) was observed. The measured data was further compared with simulated data and showed excellent agreement at all studied conditions. An equation of correlation from the simulated data is shown in Figure 5. The equation shows that laminar flame speed increases exponentially with H_2 concentration in the fuel mixture which confirms previous publications [23,24].

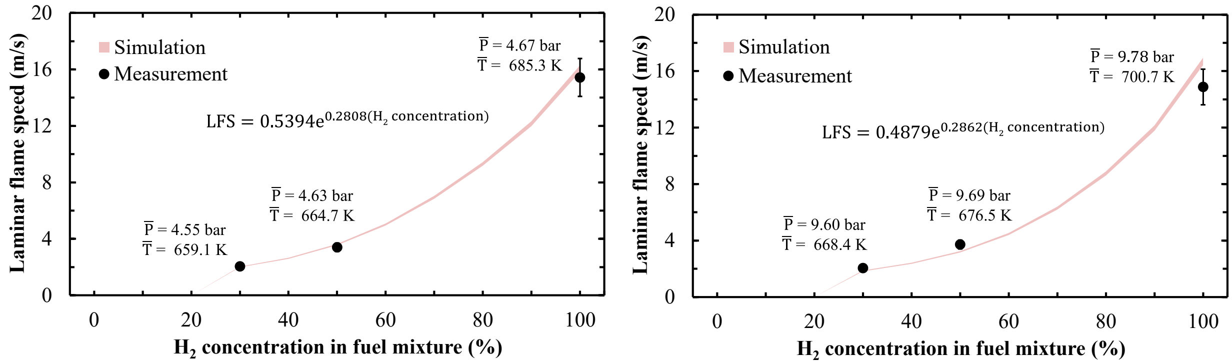

Figure 5. Measured and simulated flame speeds of NH3/H2 blends at an equivalence ratio of 1.0. The x-axis shows the hydrogen concentration in the fuel mixture. Simulations using mechanism proposed by Chen et al. [16] were shown. Mixture #1 temperature was 659K and 668K at 5 and 10bar. 665K and 676K were the temperatures at 5 and 10bar for mixture #5 from Table 1. 685K and 701K at 5 and 10bar for mixture #6 from Table 1. Measured laminar flame speed uncertainty of 8.7% and 8.5% at 5 and 10bar respectively. Simulated data has uncertainty of 2.1% and 3.2% at 5 and 10bar respectively.

4.2 Flame speeds of hydrogen flames

Three mixtures of hydrogen were used to study flame speed of hydrogen (mixtures #6, #7 and #8 from Table 1). Different mixtures were used to alter the gas temperature, as shown in Fig. 6. As temperature increases, there is a linear rise of flame speed. At both 5 and 10 bars, simulation slightly overpredicts the flame speed.

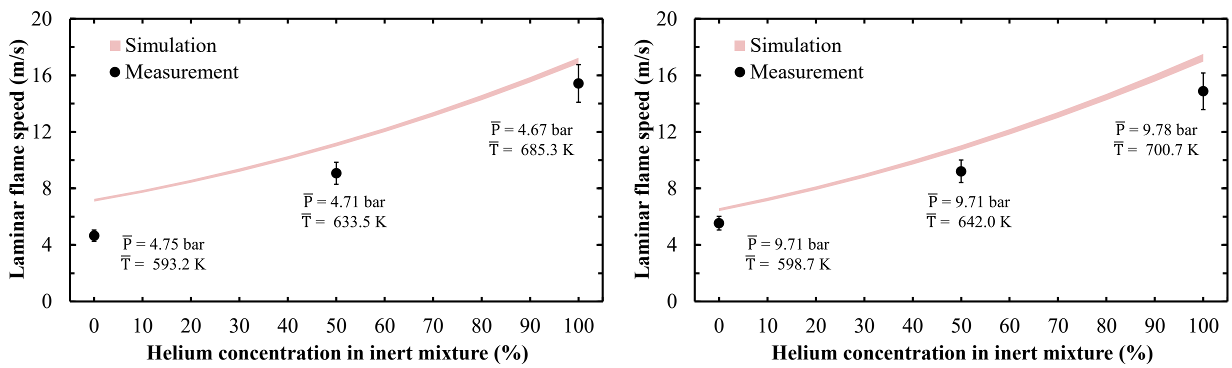

Figure 6. Measured and simulated flame speeds of hydrogen mixture at an equivalence ratio of 1.0. Simulations using mechanism of Chen et al. [16] is shown. At 593K and 599K, mixture #7 from Table 1, at 634K and 642K, mixture #8 from Table 1, and at 685K and 701K, mixture #6 from Table 1 were used. Measured laminar flame speed uncertainty of 8.7% at 5 and 10bar. Simulated data has uncertainty of 3.2% and 2.3% at 5 and 10bar respectively.

Four initial temperatures were used to study flame speed of hydrogen (mixture #6 from Table 1). Initial temperatures of 298K, 308K, 318K and 328K were used to alter the compressed gas temperature, as shown in Fig. 7. The compressed gas temperatures varied from 593.2K to 645.4K at 5bar and from 598.7K to 651.6K at 10bar. As expected, when the temperature increases, there is a linear rise of flame speed. Chen et al. mechanism was used to simulate the measured data, as shown in Fig. 7. The selected mechanism slightly overpredicts the flame speed, especially at 5bar.

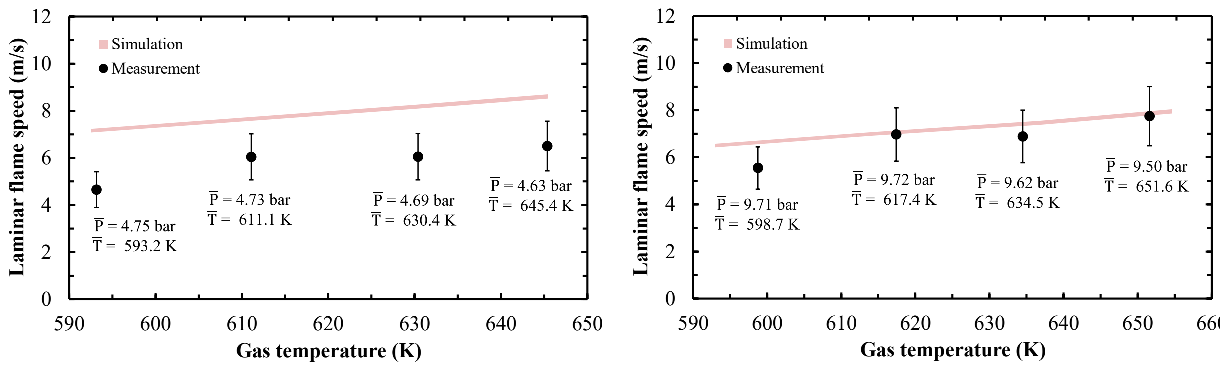

Figure 7. Laminar flame speed of hydrogen depending on compressed gas temperature at spark timing. Mixture #6 from Table 1 at 5 and 10bar. Measured laminar flame speed uncertainty of 16.2% at 5 and 10bar. Simulated data has uncertainty of 2.29% and 2.28% at 5 and 10bar respectively.

4.3 Effect of inert mixture on flame speed

To determine the impact of inert composition on flame speed, mixtures #1 to #4 were used for experiments. The initial mixture includes NH_3/H_2, helium and oxygen, exhibiting the highest flame speed. However, as the proportion of argon increased (at 50%, 75%, and 100%), a slight decrease in flame speed was observed at both 5 and 10 bar as shown in Figure 8. The mechanism of Chen et al. [15] was used for simulation and agrees well with the measurements.

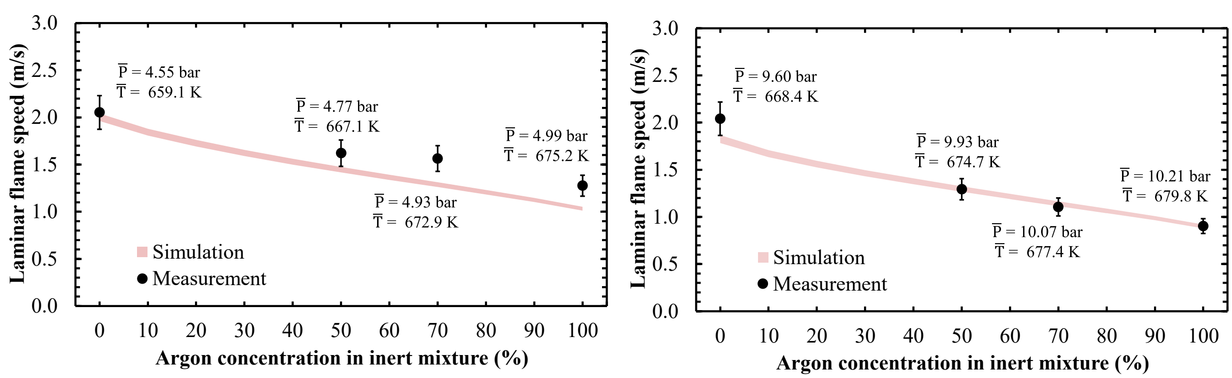

Figure 8. Flame speeds of stoichiometric NH_3/H_2 (70%/30%) blends at 5 and 10 bar. At 659K and 668K, mixture #1 from Table 1, at 667K and 675K with mixture #2, at 673K and 677K with the mixture #3, and at 675K and 680K, mixture #4 from Table 1 were used. Measured laminar flame speed uncertainty of 8.7% and 7.6% at 5 and 10bar respectively. Simulated data has uncertainty of 2.1% and 2.4% at 5 and 10bar respectively.

As shown in Fig. 8, laminar flame speed decreases while the argon concentration increases in the inert mixture. It is worth noting that the temperature of the compressed gas increases with argon concentration. The increase of temperature is due to the specific heat capacity difference between argon and helium, the latter is around a tenth of the argon's value.

The simulated mechanism matches well the measurements, especially at 10bar except for pure helium mixture which it overpredicts the flame speed. At 5bar, the mechanism is also overpredicting the laminar flame speed except with pure helium mixture. The maximum uncertainty found for the measured data was equal to 8.7% at 5bar and 7.6% at 10bar. For the simulated data, the calculated uncertainty was 2.1% at 5bar and 2.4% at 10bar.

5. Summary

The study presented in this paper offers insights into the combustion characteristics of NH_3/H_2 blends under various thermodynamic conditions, emphasizing their potential as sustainable fuel alternatives. Key findings from the experimental and simulation analyses can be summarized as follows:

- ***Increased Flame Speed with Hydrogen Addition:*** The incorporation of hydrogen into ammonia markedly increases the laminar flame speed, highlighting the synergistic effect of hydrogen in enhancing ammonia's combustion properties. This effect is particularly pronounced as the hydrogen mole fraction within the fuel blend increases, corroborating the potential of NH_3/H_2 blends in achieving higher combustion efficiencies.
- ***Temperature's Role in Flame Dynamics:*** The experimental results underscore the critical impact of temperature on the flame speed, especially for pure hydrogen flames. The study reveals a direct correlation between increased temperatures and increased flame speeds, which is further validated by the simulation data.
- ***Effect of Inert Gases:*** The study also delves into the effect of different inert gases on flame propagation, with helium and argon serving as primary examples. The results indicate that helium, due to its superior transport properties, facilitates higher flame speeds compared to argon. This observation is crucial for designing fuel blends and combustion systems, where the choice of diluent can significantly impact flame behavior.
- ***Agreement between Experimental and Simulated Data:*** The close alignment between experimental findings and simulation results, using the mechanism proposed by Chen et al., validates the reliability of this kinetic model in predicting flame behaviors of NH_3/H_2 blends. However, discrepancies observed at specific conditions suggest areas for further refinement in kinetic modeling.

In conclusion, this investigation not only enriches the understanding of NH_3/H_2 blend combustion but also highlights the critical factors influencing flame speed and stability. The promising outcomes affirm the potential of NH_3/H_2 blends as a viable, clean combustion fuel, particularly for applications demanding high efficiency and reduced environmental impact. Future research efforts should aim at refining kinetic models based on these findings and exploring the practical applications of NH_3/H_2 blends in real-world combustion systems.

6. Acknowledgements

This work supported partially by the National Science Foundation, United States, under Grant No. 2324471. Any opinions, findings, conclusions, or recommendations expressed in this material are those of the authors and do not necessarily reflect the views of the National Science Foundation. This research was also supported partially by Enginuity Power Systems, through student salary of the first Author.

References

[1] Valera-Medina A, Xiao H, Owen-Jones M, David WIF, Bowen PJ. Ammonia for power. Prog Energy Combust Sci 2018;69:63–102. https://doi.org/10.1016/j.pecs.2018.07.001.

[2] Kurata O, Iki N, Matsunuma T, Inoue T, Tsujimura T, Furutani H, et al. Performances and emission characteristics of NH3–air and NH3CH4–air combustion gas-turbine power generations. Proceedings of the Combustion Institute 2017;36:3351–9. https://doi.org/10.1016/j.proci.2016.07.088.

[3] Kobayashi H, Hayakawa A, Somarathne KDKA, Okafor EC. Science and technology of ammonia combustion. Proceedings of the Combustion Institute 2019;37:109–33. https://doi.org/10.1016/j.proci.2018.09.029.

[4] Mei B, Zhang X, Ma S, Cui M, Guo H, Cao Z, et al. Experimental and kinetic modeling investigation on the laminar flame propagation of ammonia under oxygen enrichment and elevated pressure conditions. Combust Flame 2019;210:236–46. https://doi.org/10.1016/j.combustflame.2019.08.033.

[5] Murai R, Omori R, Kano R, Tada Y, Higashino H, Nakatsuka N, et al. The radiative characteristics of NH 3 /N 2 /O 2 non-premixed flame on a 10 kW test furnace. Energy Procedia 2017;120:325–32. https://doi.org/10.1016/j.egypro.2017.07.232.

[6] Pessina V, Berni F, Fontanesi S, Stagni A, Mehl M. Laminar flame speed correlations of ammonia/hydrogen mixtures at high pressure and temperature for combustion modeling applications. Int J Hydrogen Energy 2022;47:25780–94. https://doi.org/10.1016/j.ijhydene.2022.06.007.

[7] Goldmann A, Dinkelacker F. Approximation of laminar flame characteristics on premixed ammonia/hydrogen/nitrogen/air mixtures at elevated temperatures and pressures. Fuel 2018;224:366–78. https://doi.org/10.1016/j.fuel.2018.03.030.

[8] Wang D, Ji C, Wang Z, Wang S, Zhang T, Yang J. Measurement of oxy-ammonia laminar burning velocity at normal and elevated temperatures. Fuel 2020;279:118425. https://doi.org/10.1016/j.fuel.2020.118425.

[9] Han X, Wang Z, He Y, Zhu Y, Cen K. Experimental and kinetic modeling study of laminar burning velocities of NH3/syngas/air premixed flames. Combust Flame 2020;213:1–13. https://doi.org/10.1016/j.combustflame.2019.11.032.

[10] Li J, Huang H, Kobayashi N, He Z, Nagai Y. Study on using hydrogen and ammonia as fuels: Combustion characteristics and NO x formation. Int J Energy Res 2014;38:1214–23. https://doi.org/10.1002/er.3141.

[11] Han X, Wang Z, Costa M, Sun Z, He Y, Cen K. Experimental and kinetic modeling study of laminar burning velocities of NH3/air, NH3/H2/air, NH3/CO/air and NH3/CH4/air premixed flames. Combust Flame 2019;206:214–26. https://doi.org/10.1016/j.combustflame.2019.05.003.

[12] Lhuillier C, Brequigny P, Lamoureux N, Contino F, Mounaïm-Rousselle C. Experimental investigation on laminar burning velocities of ammonia/hydrogen/air mixtures at elevated temperatures. Fuel 2020;263:116653. https://doi.org/10.1016/j.fuel.2019.116653.

[13] Shrestha KP, Lhuillier C, Barbosa AA, Brequigny P, Contino F, Mounaïm-Rousselle C, et al. An experimental and modeling study of ammonia with enriched oxygen content and

ammonia/hydrogen laminar flame speed at elevated pressure and temperature. Proceedings of the Combustion Institute 2021;38:2163–74. https://doi.org/10.1016/j.proci.2020.06.197.

[14] Chen J, Gou X. Experimental and kinetic study on the extinction characteristics of ammonia-dimethyl ether diffusion flame. Fuel 2023;334:126743. https://doi.org/10.1016/j.fuel.2022.126743.

[15] Inc. TM. Image Processing Toolbox version: 9.4 (R2022b) 2022.

[16] Goyal T, Samimi-Abianeh O. Measurement and Simulation of Autoignition-Assisted Flame Speed of N -Heptane Mixture at Elevated Gas Temperature. Ind Eng Chem Res 2023;62:8719–25. https://doi.org/10.1021/acs.iecr.3c01102.

[17] Burke MP, Chen Z, Ju Y, Dryer FL. Effect of cylindrical confinement on the determination of laminar flame speeds using outwardly propagating flames. Combust Flame 2009;156:771–9. https://doi.org/10.1016/j.combustflame.2009.01.013.

[18] Piehl JA, Samimi-Abianeh O. Measuring the Adiabatic Ignition Delay of n-Pentane Mixture using Rapid Compression Machine. Journal of Thermal Science 2020:1–9. https://doi.org/10.1007/s11630-020-1346-7.

[19] R. J. Kee, F. M. Rupley, J. A. Miller, M. E. Coltrin, J. F. Grcar, E. Meeks, H. K. Moffat, A. E. Lutz, G. DixonLewis, M. D. Smooke, J. Warnatz, G. H. Evans, R. S. Larson, R. E. Mitchell, L. R. Petzold WCR, M. Caracotsios, W. E. Stewart, P. Glarborg, C. Wang and OA. PREMIX CHEMKIN-PRO 2023 R1 n.d.

[20] da Rocha RC, Costa M, Bai X-S. Chemical kinetic modelling of ammonia/hydrogen/air ignition, premixed flame propagation and NO emission. Fuel 2019;246:24–33. https://doi.org/10.1016/j.fuel.2019.02.102.

[21] Mathieu O, Petersen EL. Experimental and modeling study on the high-temperature oxidation of Ammonia and related NOx chemistry. Combust Flame 2015;162:554–70. https://doi.org/10.1016/j.combustflame.2014.08.022.

[22] Chemkin-Pro: Chemistry Effects Predicting Simulation Software | Ansys n.d. https://www.ansys.com/products/fluids/ansys-chemkin-pro (accessed January 29, 2021).

[23] Pessina V, Berni F, Fontanesi S, Stagni A, Mehl M. Laminar flame speed correlations of ammonia/hydrogen mixtures at high pressure and temperature for combustion modeling applications. Int J Hydrogen Energy 2022;47:25780–94. https://doi.org/10.1016/j.ijhydene.2022.06.007.

[24] Shrestha KP, Lhuillier C, Barbosa AA, Brequigny P, Contino F, Mounaïm-Rousselle C, et al. An experimental and modeling study of ammonia with enriched oxygen content and ammonia/hydrogen laminar flame speed at elevated pressure and temperature. Proceedings of the Combustion Institute 2021;38:2163–74. https://doi.org/10.1016/j.proci.2020.06.197.